Antiviral Research 161 (2019) 154–162

Contents lists available at ScienceDirect

Antiviral Research

journal homepage: www.elsevier.com/locate/antiviral

Research paper

A synthetic glycosaminoglycan mimetic blocks HSV-1 infection in human iris stromal cells

Hardik Majmudar[a], Meng Hao[a], Nehru Viji Sankaranarayanan[b], Brian Zanotti[a], Michael V. Volin[a], Umesh R. Desai[b], Vaibhav Tiwari[a,*]

[a] Department of Microbiology & Immunology, College of Graduate Studies, Midwestern University, Downers Grove, IL 60515, USA
[b] Department of Medicinal Chemistry and Institute for Structural Biology, Drug Discovery and Development, Virginia Commonwealth University, Richmond, VA 23219, USA

A B S T R A C T

Herpes simplex virus type-1 (HSV-1) is a significant pathogen that affects vision by targeting multiple regions in the human eye including iris. Using a focused library of synthetic non-saccharide glycosaminoglycan mimetics (NSGMs), we identified sulfated pentagalloylglucoside (SPGG) as a potent inhibitor of HSV-1 entry and cell-to-cell spread in the primary cultures of human iris stromal (HIS) cells isolated from eye donors. Using *in vitro* β-galactosidase reporter assay and plaque reduction assay, SPGG was found to inhibit HSV-1 entry in a dosage-dependent manner (IC_{50} ~6.0 μM). Interestingly, a pronounced inhibition in HSV-1 entry and spread was observed in HIS cells, or a cell line expressing specific gD-receptor, when virions were pre-treated with mimetics suggesting a possible interaction between SPGG and the HSV-1 glycoprotein. To examine the significance of gD-SPGG interaction, HIS cells were pretreated with SPGG, which showed a significant reduction in gD binding. Taken together, our results provide strong evidence of SPGG being a novel viral entry inhibitor against ocular HSV infection.

1. Introduction

Herpes simplex virus type-1 (HSV-1) infection poses significant threat towards visual impairment and vision loss by infecting ocular cells and tissues including the regions of iris (Zhu and Zhu, 2014; Dawson and Togni, 1976). It has been shown that inflammation of the iris following HSV-1 infection may be associated with elevated intraocular pressure, which may result in glaucoma, although the possibility remains that this may be steroid-induced (Tugal-Tutkun et al., 2010; Teitelbaum et al., 1987; Rathinam and Namperumalsamy, 2007; Sungur et al., 2010; Van der Lelij et al., 2000). Further, iris has also been shown to have histopathologic involvement in HSV-1 infection of the corneal stroma, herpetic stromal keratitis (HSK) (Tugal-Tutkun et al., 2010). Inflammation of the iris is also seen in herpetic anterior uveitis, a condition that often presents as an inflammation of the iris and ciliary body (iridocyclitis) and is the leading cause of infectious anterior uveitis worldwide (Rathinam and Namperumalsamy, 2007). Using primary cultures of human iris stromal (HIS) cells derived from human eye donors, we previously reported on the susceptibility of HIS cells to HSV-1 infection including molecular expression of viral entry receptors and the associated inflammatory mediators (Baldwin et al., 2013).

The early phase of HSV-1 infection starts when the viral envelope glycoproteins interact with their respective host cell receptors (Spear and Longnecker, 2003). During the initial attachment step virus glycoprotein B (gB) and glycoprotein C (gC) interacts with host cell surface heparan sulfate proteoglycans (HSPGs) (WuDunn and Spear, 1989; Herold et al., 1991; Shieh et al., 1992). A second proposed step involves virus surfing along the filopodia utilizing heparan sulfate (HS) chain (Oh et al., 2010). Following viral binding and surfing, a third HSV-1 glycoprotein called glycoprotein D (gD) interacts with one or more of the host cell receptors, such as nectin-1, herpesvirus entry mediator (HVEM) (Montgomery et al., 1996), or 3-*O*-sulfated heparan sulfate (3-*O*S HS) (Shukla et al., 1999; Shukla and Spear, 2001) to induce cellular entry. In this process, gD undergoes a conformational change, which helps it associate with the heterodimer complex of glycoprotein H-glycoprotein L (gH-gL). The latter event is followed by gH-gL binding to gB, which allows the viral and host cell membranes to fuse (Krummenacher et al., 2013; Eisenberg et al., 2012).

In this current study, we reasoned that HSV-1 entry and spread could be prevented by non-saccharide glycosaminoglycan mimetics (NSGMs), a group of molecules that attempt to mimic the structure and/or function of heparan sulfate (Desai, 2013; Al-Horani et al., 2013; Patel et al., 2014; Al-Horani et al., 2015). Using human iris stromal (HIS) cells and gD-receptor specific cells, we show that a specific NSGM, called sulfated pentagalloylglucoside (SPGG), is a potent inhibitor of HSV-1 entry and cell-to-cell spread. This work presents the proof-of-concept and highlights the promise of SPGG in its further development

* Corresponding author.
E-mail address: vtiwar@midwestern.edu (V. Tiwari).

https://doi.org/10.1016/j.antiviral.2018.11.007
Received 15 August 2018; Received in revised form 9 November 2018; Accepted 15 November 2018
Available online 24 November 2018
0166-3542/

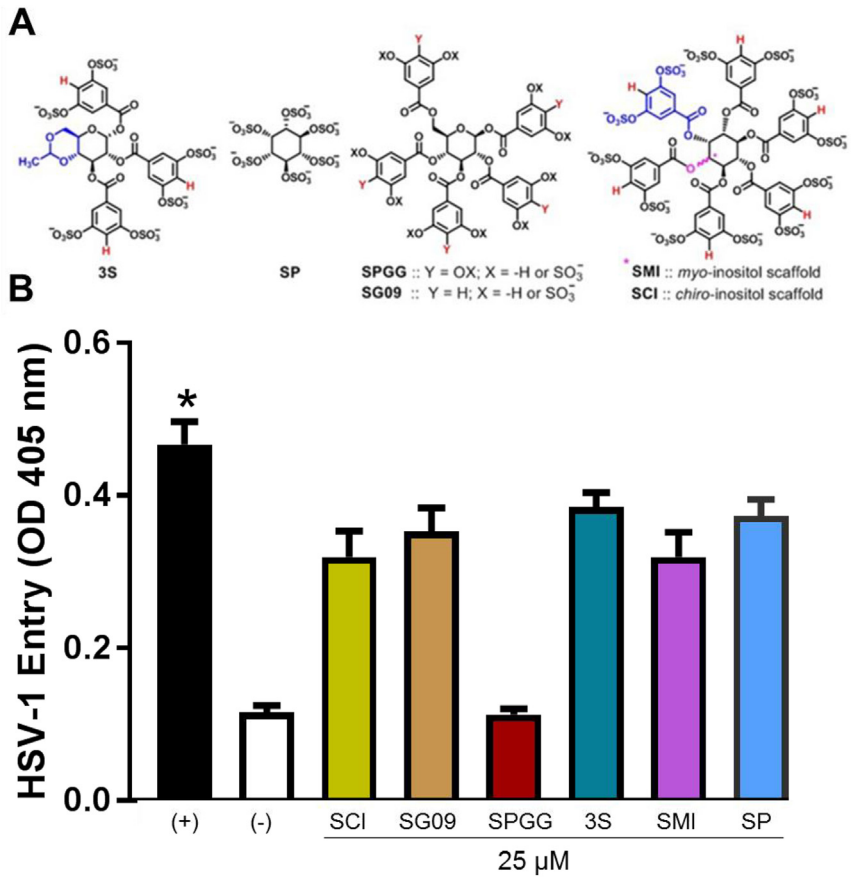

Fig. 1. (A). The focused library of non-saccharide glycosaminoglycan mimetics (NSGMs) used to discover anti-HSV-1 agents. The library consists of 3S, SP, SPGG, SG09, SMI and SCI, which were chemically synthesized. The sulfated nature of heparan sulfate is mimicked by the presence of multiple sulfate groups on these molecules (numbering six to twelve) and stereochemically different orientation arising from the scaffold and substitution pattern. **(B). Effect of the NSGM library screening on HSV-1 entry.** African monkey kidney (Vero) cells plated in 96-well plates were pre-incubated with 25 μM individual compounds of the library or mock treated for 45 min at room temperature. The cells were then challenged with β-galactosidase-expressing recombinant HSV-1(KOS) gL86 at 37 °C. Enzymatic activity of β-galactosidase expression was evaluated by using ONPG (*o*-nitrophenyl-D-galactopyranoside) assay at 405 nm of optical density. The values shown represent the amount of reaction product detected spectrophotometrically at a single input dose of 1 multiplicity of infection (MOI). Untreated positive (+) control and HSV-1 uninfected negative (−) controls are expressed. Data represent the mean ± the standard deviation of results in triplicate wells in a representative experiment. The experiment was repeated three times with similar results.

as a potential therapeutic against ocular HSV infection.

2. Results

2.1. Screening a library of non-saccharide glycosaminoglycan mimetics (NSGMs) against HSV-1 infection

To target initial event of HSV-1 attachment/binding to prevent infection, we used a library of NSGMs, which included 3S, SP, SPGG, SG09, SMI, and SCI (Fig. 1A). These molecules were chemically synthesized, as reported earlier (Patel et al., 2014). Structurally, three of these molecules have a central domain of glucopyranose moiety (3S, SPGG, and SG09), while the remaining are based on a related scaffold called inositol (SP, SMI, and SCI). The number of sulfate groups varies from six (e.g., 3S and SP) to twelve (e.g., SMI and SCI) with SPGG and SG09 containing 10 groups. Stereochemically, each NSGM differs considerably from others in the group and therefore, heparan sulfate-like 'pharmacophore' presented by each NSGM is strikingly different. Thus, although the library is small, the diversity of structures is much higher, which enhances the probability of identifying an inhibitor.

We started our initial screening using above candidates in African green kidney monkey (Vero) cells. The cells were pre-treated with a NSGM at 25 μM concentration for 60 min at room temperature before the β-galactosidase expressing reporter HSV-1 (KOS) gL86 challenge at 1 multiplicity of infection (MOI) for 6 h. Viral entry assays were based on quantification of HSV infection-induced viral β-galactosidase expression using ONPG (*o*-nitrophenyl-D-galactopyranoside (ImmunoPure, Pierce) assay. Expression levels of β-galactosidase are induced by HSV infection and therefore is used as a measureable indicator of viral entry (Montgomery et al., 1996; Tiwari et al., 2006). As shown in Fig. 1B, pre-incubation with SPGG significantly inhibited HSV-1 entry compared to the other tested analogs. These results provide initial evidence for the potential of SPGG as a specific anti-viral entry agent. Further confirmation of HSV-1 entry inhibition was established using x-gal (5-bromo-4-chloro-3-indolyl-β-D-galactosidase, Sigma) staining (data not shown). Interestingly SPGG has been previously shown to have potent anticoagulant activity by inhibiting factor XIa through binding to its GAG binding site(s) (Al-Horani et al., 2013; Al-Horani et al., 2015; Al-Horani and Desai, 2014).

2.2. Inhibition of HSV-1 entry by SPGG in primary cultures of human iris stromal (HIS) cells

Since HSV-1 is known to infect and replicate in human iris stromal (HIS) cells (Baldwin et al., 2013), we next examined the potential of SPGG in preventing HSV-1 entry in a clinically relevant cell line. Primary cultures of HIS cell were prepared in accordance with institutional review board-approved protocols and were isolated from anonymously donated human eyes (provided by the Illinois Eye Bank, Chicago, IL) via sterile dissection of the iris and pigmented epithelial layer and subsequent removal with a sterile cotton swab. The tissue was then digested with 0.2% type II collagenase (Sigma-Aldrich, St. Louis, MO) in cell culture medium, MCDB-131 (Sigma-Aldrich, St. Louis, MO) at 37 °C with gentle stirring for 20–30 min. Digested tissues were next centrifuged to remove tissue debris, and HIS cells were cultured in MCDB-131 containing 10% fetal bovine serum (FBS) and antibiotics.

Cultured HIS cells were pre-treated with SPGG analog or mock-treated in a dosage dependent manner followed by infection with recombinant form of HSV-1 (KOS) gL86 that expresses β-galactosidase under the HSV-1 immediate-early promoter following cell entry (Shukla et al., 1999). Mock infection with PBS was used as a negative control. As shown in Fig. 2A, compared to the negative uninfected control, SPGG treatment of HIS cells demonstrated inhibition of viral entry in a dose-dependent manner. We further confirmed the above-described

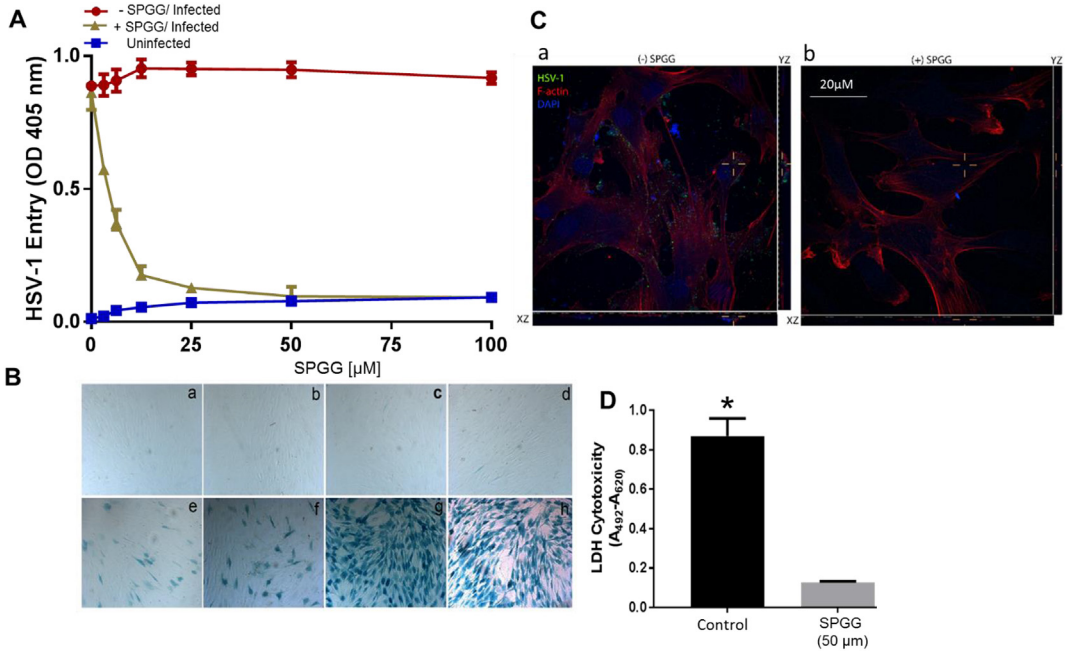

Fig. 2. SPGG-mediated inhibition of HSV-1 entry into primary cultures of human iris stromal (HIS) cells. (A). HIS cells plated in 96-well plates and inoculated with two-fold serial dilutions of SPGG followed by β-galactosidase-expressing recombinant HSV-1(KOS) gL86 virus. After 6 h, the cells were permeabilized and incubated with ONPG substrate for quantitation of β-galactosidase activity at OD_{410}. Data represent the mean ± the standard deviation of results in triplicate wells in a representative experiment. The experiment was repeated three times with similar results. **(B).** SPGG mediated blocking of HSV-1 entry into HIS cells was confirmed by × -gal staining. Dosage dependent pretreatment of HIS cells with SPGG (a: 100 μM, b: 50 μM, c:25 μM, d:12.5 μM, e:6.1 μM, f:3.1 μM, g:1.5 μM, h: mock-treated) followed by a challenge with β-galactosidase-expressing recombinant HSV-1 (gL86) at 1 MOI. Mock-treated HIS cells and uninfected HIS cells were used as positive and negative controls, respectively. Blue cells were seen as shown. Microscopy was performed using the magnification of 20 × objective of a Zeiss Axiovert 100. **(C). High resolution confocal microscopy demonstrating inhibition of HSV-1 entry into HIS cells treated with SPGG.** Confluent monolayers of cultured HIS cells (0.5×10^6) on cover glass were mock treated or treated with SPGG (50 μM) for 60 min followed by infection with HSV-1 KOS (K26GFP) at 5 MOI. After 60 min, cells were washed in phosphate-buffered saline (PBS) and fixed. The cells were stained with 4′, 6′-diamidino-2-phenylindole (DAPI) and red-phalloidin examined under three separate channels (FITC, DAPI and cy3) and merged. Panel a shows the large number of green virions localization on cell membrane as well internalized in the mock-treated cells. Panel b shows only few virus particles in the membrane area in HIS cells treated with SPGG. The images were obtained using Nikon Elements software on a Nikon A1R confocal inverted microscope system. The picture was produced and processed in Adobe Photoshop 7.0. **(D).** Cytotoxic effect of SPGG on HIS cells. The HIS cells monolayers were incubated in the presence and absence of SPGG at 50 μM. After 24 h of incubation at 37 °C cell toxicity was determined by the LDH assay. Asterisks indicate significant difference from controls ($P < 0.05$, *t*-test), error bars represent SD from a triplicate experiments.

result via × -Gal (5-bromo-4-chloro-3-indolyl-β-d-galactopyranoside) staining after infecting HIS cells with the reporter HSV-1. As shown in Fig. 2B, cultured HIS cells that were pre-treated with SPGG (6.1–100 μM) and then exposed to HSV-1 (KOS) gL86 significantly lost the blue color (Fig. 2B, panels a–e) compared to untreated HIS cells (Fig. 2B, panel h).

2.3. Visualization of HSV-1 infectivity in HIS cells in presence of SPGG by confocal microscopy

We next used confocal microscopy to visualize HSV-1 infection in HIS cells in presence of SPGG (50 μM). A green fluorescent protein (GFP)-capsid tagged HSV-1 (K26-GFP) virus (5 MOI) was used for infection. The cells were fixed 60 min post infection and stained with tetramethyl rhodamine isocyanate (TRITC)-conjugated phalloidin binding to F-actin, as previously described (Tiwari et al., 2006). As shown in Fig. 2C, a majority of the cultured HIS cells infected with HSV-1 without SPGG treatment showed a large number of punctate green fluorescence surrounding the DAPI-stained blue nucleus and at the membrane (Fig. 2C, panel a). Z-stacking of the HSV-1 infected HIS cells demonstrated the internalization of HSV-1 virions (Fig. 2C, panel a). In contrast, SPGG treated HIS cells showed significantly loss of GFP particles inside the cells (Fig. 2C, panel b). Taken together, the results from imaging experiment along with quantitative ONPG assay established the role of SPGG as a potent viral entry inhibitor. Finally, the impact of SPGG on cellular toxicity was determine using an LDH assay which related that SPGG at 50 μM concentration was nontoxic to HIS cells (Fig. 2D).

2.4. SPGG significantly blocks HSV-1 entry in gD-receptor expressing cells

Next we evaluated the broader significance of SPGG as an anti-HSV agent. We therefore, tested the ability of SPGG to block viral entry using F strain. Here we used nectin-1 expressing CHO Ig8 cells that express β-galactosidase upon viral entry (Montgomery et al., 1996). In this experiment, virus pre-incubated with SPGG (50 μM) was used to infect the cells at 1 MOI. The results showed that SPGG blocked entry of HSV-1 F strain as evident by the ONPG-based entry assay (Fig. 3A) suggesting the antiviral activity of SPGG is not restricted to KOS strain. Since, HIS cells are known to express all the known gD-receptors (Baldwin et al., 2013), therefore next, we determined the if the inhibitory effect of SPGG against HSV-1 entry was specific to a gD-receptor. Chinese hamster ovary (CHO-K1) cells expressing individual gD receptor (nectin-1, HVEM or 3-*OST*-3) were pre-treated with SPGG (10 μM) or mock treated for 60 min followed by infection with β-galactosidase expressing HSV-1 reporter virus (gL86). As shown in Fig. 3B, pre-treatment with SPGG significantly blocked HSV-1 entry in a dose dependent manner in gD receptor expressing CHO-K1 cells. As expected, the control cells treated with 1 × PBS (untreated) showed HSV-1 entry. This data suggest that SPGG blocks HSV-1 entry in target cells expressing any gD-receptors.

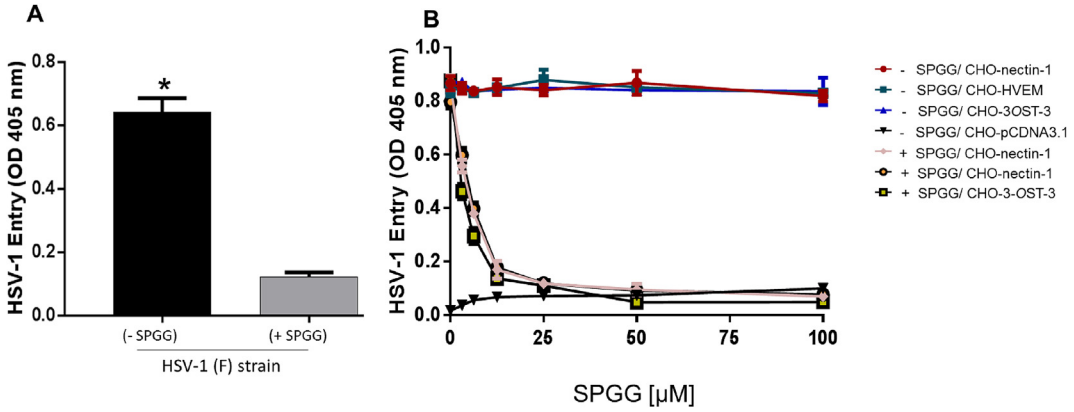

Fig. 3. (A). HSV-1 entry blocking activity of SPGG against HSV-1 (F) strain. The HS-mimetic (SPGG; 50 μM) was pre-incubated with HSV-1 (F) strains of HSV-1 at 1 MOI for 1 h at 37 °C. The CHO Ig8 cells infected with HSV-1 (F-strain) alone in absence of SPGG was used as control. Viral entry was measured by ONPG assay. Asterisks indicate significant difference from controls ($P < 0.05$, *t*-test), error bars represent SD from a triplicate experiments. **(B). Dose-response analysis of SPGG on HSV-1 entry into Chinese hamster ovary (CHO-K1) cells expressing individual gD-receptor (nectin, HVEM and 3-*OST*-3).** CHO-K1 cells expressing nectin-1, HVEM ndd 3-*OST*-3 were plated in 96-well plates and inoculated with two-fold serial dilutions of SPGG or mock-treated followed by β-galactosidase-expressing recombinant HSV-1(KOS) gL86 virus at 1 MOI. CHO-K1 cells expressing pCDNA3.1 infected with HSV-1 was used as a negative control. After 6 h, the cells were permeabilized and incubated with ONPG substrate for quantification of β-galactosidase activity expressed from the input viral genome. Enzymatic activity was measured by determining OD 405 nm. Data represent the mean ± the standard deviation of results in triplicate wells in a representative experiment. The experiment was repeated three times with similar results.

2.5. Kinetics of inhibition by SPGG during HSV-1 spread by plaque reduction assay

Next, we investigated the effect of SPGG on viral replication and spread to the neighboring cell. In this experiment, we used a recombinant form of HSV-1 (KOS) 804, a mutant known to form high numbers of syncytia (Little and Schaffer, 1981). The HIS cells were pre-incubated with SPGG and then challenged with HSV-1 (KOS) 804 at MOI of 0.01 for 2 h at 37 °C. The cells were infected from 12 to 48 h. At a given time point, cells were washed with PBS buffer, fixed in fixative buffer, and stained with Giemsa stain for visualization and quantification of number of plaques formed. As shown in Fig. 4A (panels a to d), large number plaques were visualized at greater lengths of time post-infection (p.i.), while no plaques were observed in the mock-infected control or HIS cells treated with SPGG infected with HSV-1 (KOS) 804 strain. Upon quantification, the number of plaques increased with time in untreated and HSV-1 infected HIS cells, while no plaque was observed till 48 h (Fig. 4B). These results, together with those of the entry assay, show that SPGG negatively affects both viral entry and viral spread in primary cultures of HIS cells.

2.6. SPGG interacts with HSV-1 envelope glycoprotein

We next determined whether the inhibitory activity of SPGG on HSV-1 entry was attributed to target cells or viral particles. HIS cells and the Chinese hamster ovary (CHO-K1) cells expressing individual gD-receptor (nectin-1, HVEM and 3-*OST*-3) were pre-incubated with SPGG (10 μM) or mock treated with 1 × PBS for 60 min followed by challenge to HSV-1 infection at 1 MOI. In parallel, HSV-1 (KOS) gL86 virions (1 MOI) were pre-incubated with SPGG (10 μM) for 60 min before infection to tbe target cells. Interestingly, as shown in Fig. 5 (A-D), pre-incubation of SPGG with virus had significant inhibition of HSV-1 entry compare to cell incubation suggesting that anti-HSV-1 activity of SPGG is mostly due to the effect on viral particles.

2.7. Pre-incubation of SPGG with HSV-1 glycoprotein expressing effector cell significantly impairs cell fusion

During HSV pathogenesis, the virus uses a strategy to avoid evading immune system by infecting the neighboring cells without diffusing through the extracellular environment (Sattentau, 2008; Fischer et al., 2001). The mechanism of virus spread from cell-to-cell is mediated through the coordinated efforts of surface exposed glycoproteins from infected cells that contact their specific receptors on neighboring uninfected cells. It has been shown that, similar to the membrane fusion that occurs during entry, cells expressing HSV-1 glycoprotein's gB, gD, gH, and gL fuse with cells expressing gD receptors (Atanasiu et al., 2010), and thus cell-to-cell fusion mimics the minimum requirement for entry.

To verify that SPGG indeed prevented the membrane fusion that occurs during HSV-1 entry, we used a quantitative and efficient cell-to-cell fusion assay (Tiwari et al., 2004; Tiwari et al., 2007). It has been shown that, similar to the membrane fusion that occurs during entry, cells expressing HSV-1 glycoprotein's gB, gD, gH, and gL fuse with cells expressing gD receptors (Atanasiu et al., 2010), and thus cell-to-cell fusion mimics the minimum requirement for entry. In our experiment, wild type CHO-K1 cells were transiently transfected with each of four HSV-1 glycoproteins(gBgD, gHand gL, as well as, the plasmid pT7EM-CLuc that expresses a luciferase reporter gene was considered “effector” cell. In parallel “target” HIS cells or CHO-K1 cells transiently expressing nectin, HVEM and 3-*OST*-3 enzyme as gD receptor(s) were separately transfected with the plasmid pCAGT7, which expresses T7 RNA polymerase to induce expression of the Luciferase gene. For a negative control, effector cells were transfected with T7 RNA polymerase and control plasmid pcDNA3.1. In our experiment either target cells expressing gD-receptor or effector cells expressing HSV-1 glycoproteins were pre-treated with SPGG at 10 μM for 60 min before mixing both cell-types. As expected a high amount of fusion occurred between mock-treated effector and target cells [CHO-HIS, CHO-CHO-nectin, CHO-CHO-HVEM, and CHO-CHO-3-OST-3] (positive controls) compared to the pcDNA3.1 expressing CHO effector cells (negative control) (Fig. 6). Target HIS cells expressing naturally gD-receptor(s) or transiently expressing CHO-K1 cells upon pre-treatement to SPGG (10 μM) before mixing to the effector cells significantly impaired the cell fusion (Fig. 6; bar a). However, the maximum inhibitory effect of SPGG was noticed when effector cells were pre-incubated with SPGG (Fig. 6; bar b).

We further confirmed the above results by visualizing multi-nucleated giant cells or syncytia formation as a means of viral spread (Tiwari et al., 2007). A similar trend was observed as SPGG pre-treatment either to a target cells or effector cells significantly inhbited syncytia formation. Again, higher inhibition in terms of the number and

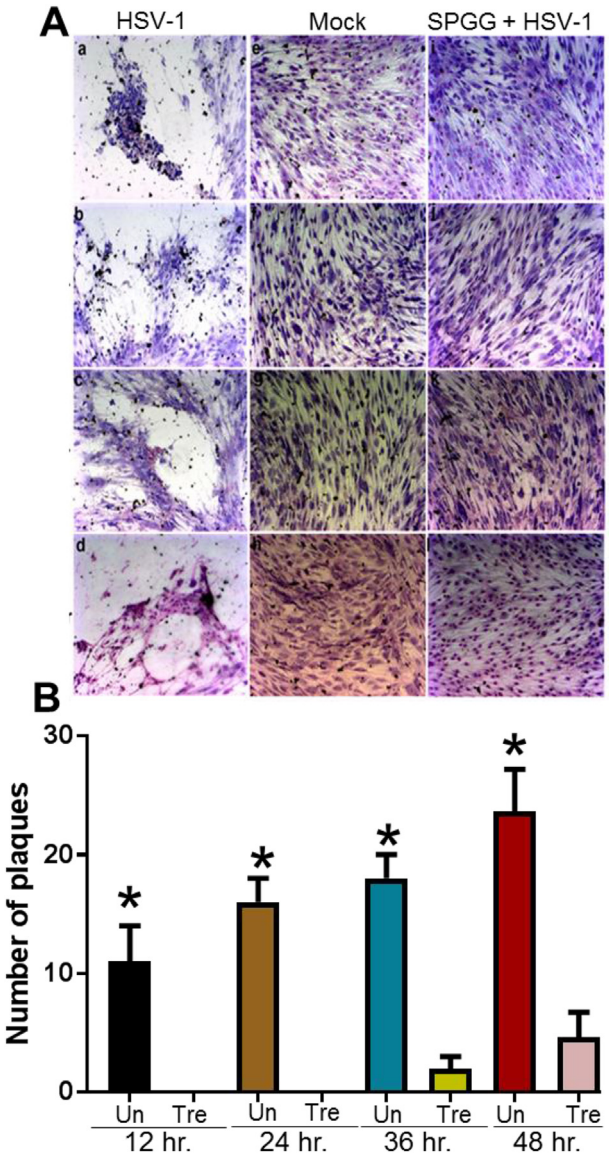

Fig. 4. Imaging and quantification of HSV-1 plaque formation in cultured HIS cells in presence and absence of SPGG. (A). Confluent monolayers of HIS cells pretreated with SPGG or mock treated at 10 μM for 60 min were infected with HSV-1 (KOS) 804 strain for 2 h. The plaque formation was imaged at (a) 12 h, (b) 24 h, (c) 36 h, (d) 48 h post infection and quantified the number of plaques formed in presence and absence of SPGG in triplicate experiments (panel B). In parallel, mock infected HIS cells were used as a negative control. The images were taken with a Zeiss Axiovert 100 microscope at 20× magnification. Asterisks indicate significant difference from controls ($P < 0.05$, *t*-test), error bars represent SD from a triplicate experiments.

size of visual multi-nucleated giant cells was observed when effector cells were pre-incubated with SPGG compared to target cells (data not shown). These results reinforce our findings that SPGG thus potentially act on HSV-1 glycoprotein.

2.8. SPGG impairs HSV-1 glycoprotein D (gD) binding to HIS cells

Finally, we analyzed the impact of SPGG on HSV-1 gD binding cells. We reasoned whether a soluble recombinant form of HSV-1 gD-Fc would bind cultured HIS cells and whether this binding could be adversely affected in the presence of SPGG using cell enzyme-linked immunosorbent assay, as previously described by us (Tiwari et al., 2006). HIS cells either treated with SPGG (10 μM) or mock-treated were allowed to bind equal amount of gD (1 μg/mL), and binding was detected with a spectrophotometer. In parallel experiment, soluble gD-Fc were also pre-incubated with SPGG (10 μM) for 60 min before treating the HIS cells. As shown in Fig. 7A, gD binding to mock-treated HIS cells was not affected, however, the binding of gD to SPGG-treated HIS cells was drastically reduced (Fig. 7A; bar a). Interestingly, even a significant loss of gD was noticed when gD was pre-incubated with SPGG (Fig. 7A; bar b). This finding strongly supports that SPGG interacts with gD, a critical viral glycoprotein which mediates its receptor interaction to facilitate viral entry.

The reason why SPGG interacts with gD can be understood through calculation of surface electrostatics of gD (Fig. 7B). This shows presence of two strongly electropositive domain, which can interact favorably with SPGG. In fact, the crystal structure also shows a sulfate moiety, most probably from the buffer, trapped in this electropositive domain. Finally, our recent studies using spectrofluorimetry show that SPGG binds gD with high affinity (~10 nM) (Gangji et al., 2018).

3. Discussion

Our recent study identified SPGG, a NSGM family member as a new class inhibitor which blocks HSV-1 entry in HeLa cell (Gangji et al., 2018). By testing its ability to block HSV-1 entry and spread in gD receptor cells including primary cultures of HIS cells, we have demonstrated the clinical relevance of SPGG analogs for the future drug development against ocular HSV-1 infection. The concentration of SPGG used in this study were non-toxic to cells as previously reported in multiple other cell-types (Gangji et al., 2018). In addition, SPGG shows major promise by reducing HSV-1 cell-to-cell fusion in HIS cells. The later step is critical in viral spread and associated inflammatory damage.

From a mechanistic view point, pre-incubation of SPGG with the target cells or with the virions clearly demonstrated drastic reduction in HSV-1 entry and cell-to-cell spread. Similar results obtained from our imaging experiment. The effectiveness of this analog is not just limited to preventing viral entry, but also as an agent that effectively blocks viral spread as evident from plaque reduction assay. We also investigated the role SPGG played in cell-to-cell viral spread and virus-induced membrane fusion. Through both, reduction in viral entry assay as well as in plaque reduction formation assay, we concluded that the presence of SPGG inhibited both entry and cell-to-cell spread of HSV-1 (Figs. 2–4). These results were later confirmed with a virus free cell-to-cell fusion assay (Fig. 5). In addition, SPGG showed even a higher impact when pre-treated with virus and gD-binding to HIS cells.

The above property of small molecule SPGG makes it a promising product for HSV-1 antiviral therapy. Its ability to prevent cell-to-cell spread also makes it of specific interest in the development of low cost prophylactics having the potential to treat an existing infection as well. Given the fact that anti-HSV resistance increasing against the existing drugs such as acyclovir (Wilson et al., 2009), the development of new class of therapeutics is in great demand, especially, which are readily available, non-toxic to cells and can easily be synthesized at low cost. We believe that our discovery of NSGMs as anti-HSV agents will have a good impact in the field of therapeutics. These results highlight both the prophylactic and neutralization ability of SPGG to suppress HSV-1 infection in ocular cell culture model.

SPGG is a synthetic agent. Its synthesis was achieved in less than 5 steps, which bodes well for development of SPGG as a drug itself. A major opportunity for therapeutic application of this novel agent is to develop a topical solution. Considering that SPGG is a highly water soluble, appropriate polymer – SPGG preparation could be developed as s topical cream to prevent infection in a prophylactic manner. Another major opportunity is to develop better SPGG analogs. Numerous structural derivatives of SPGG can be prepared and studied for this binding to gD. Following analysis of target specificity, binding affinity, dosage requirement and toxicity, a promising SPGG analog could be

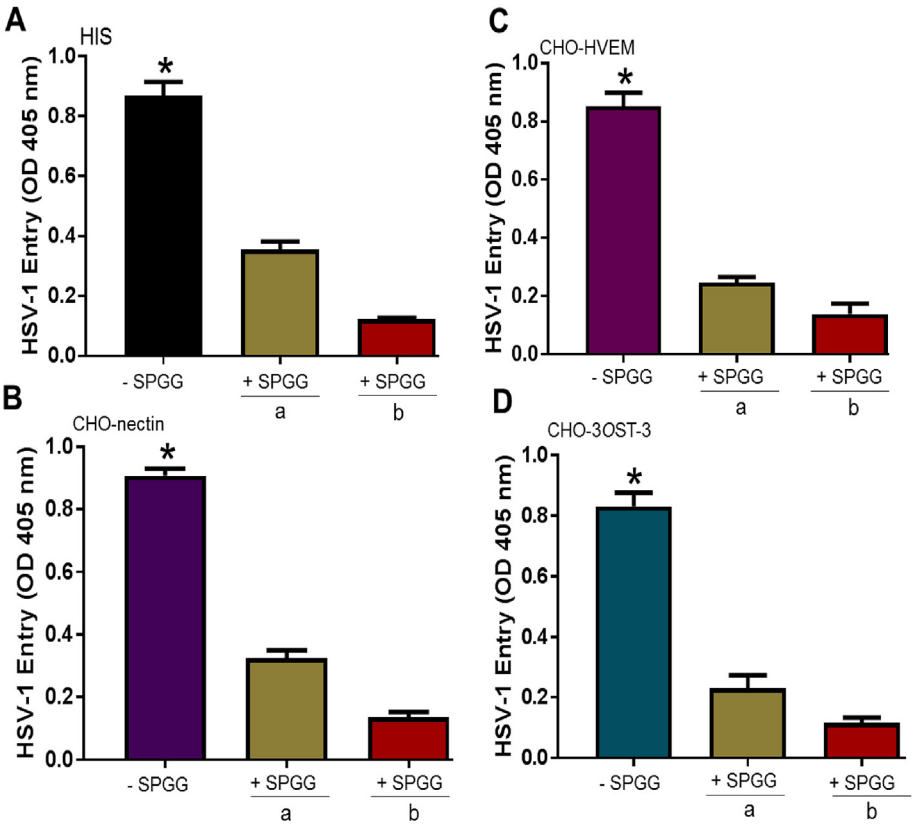

Fig. 5. Pre-incubation of SPGG with HSV-1 significantly inhbited viral entry. Confluent monolayers of HIS cells (panel A) or CHO-K1 cells expressing nectin-1 (panel B), HVEM (panel C), and 3-OST-3 (panel D) were mock treated or treated with SPGG at 10 μM for 60 min (bar a) before challenged with HSV-1 (KOS) gL86 virus at 1 MOI for 60 min. In parallel, SPGG (10 μM) was pre-incubated with HSV-1 (KOS) gL86 virus at 1 MOI before challenging to cells (bar b). After 6 h, the cells were permeabilized and incubated with ONPG substrate for quantification of β-galactosidase activity expressed from the input viral genome. Enzymatic activity was measured by determining OD 405 nm. Data represent the mean ± the standard deviation of results in triplicate wells in a representative experiment. Asterisks indicate significant difference from controls ($P < 0.05$, *t*-test), error bars represent SD from a triplicate experiments. The experiment was repeated three times with similar results.

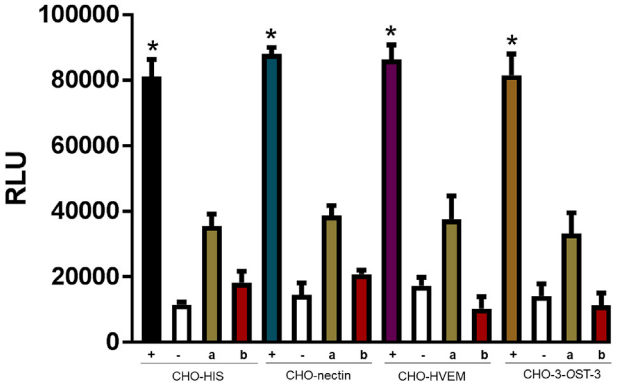

Fig. 6. Pre-treatment of SPGG with effector cells inhibits HSV-1 glycoprotein mediated cell-to-cell fusion. The effector CHO-K1 cells co-expressing HSV-1 glycoproteins (gB, gD, gH-gL) and T7 Polymerase pretreated with SPGG 10 μM before mixing with target cells (b bars). The target cells in the experiment were HIS cells which naturally expresses gD-receptors or CHO-K1 cells co-expressing luciferase gene along with gD-receptor (nectin-1, HVEM, 3-*O*ST-3). In paralle experiment, target cells were pre-treated with SPGG before mixing with effector cells (a bars). The SPGG untreated effector and target cells were used as a positive (+) control. Effector cells without glycoproteins were considered the negative (−) control (empty bar). Membrane fusion as a means of viral spread was detected by monitoring luciferase activity 24 h after co-cultivating the effector and target cells. Relative luciferase units (RLUs) were determined using a Sirius luminometer (Berthold detection systems) and are from three independent experiment per-formed in triplicate. Error bars represent standard deviations. *$P < 0.05$, one-way ANOVA.

taken up in a clinical setting.

HS mimetics are already proving to be very useful in antagonizing chemotactic activity of pro-inflammatory cytokines (Sheng et al., 2013) and as an anti-angiogenic molecules (Jayson et al., 2014; Ferro et al., 2007; Dredge et al., 2010; Raman et al., 2012), both of which are associated with herpetic stromal keratitis (HSK) and corneal neovascularization during ocular HSV-1 infection which leads to vision loss (West et al., 2014; Todd et al., 2011). Therefore, such small molecules can be valuable candidate in preventing not only HSV-1 entry but as well as moving inflammatory cells in response to HSV-1 in ocular cells and tissues. To further develop SPGG as a topical drug candidate, screening in an *in vivo* or *ex-vivo* eye disease model (Tiwari et al., 2011) of HSV-1 infection will be required. Similarly, evaluating the profiles of inflammatory markers in corneas in presence of SPGG and its impact on heparanase activity will also be very useful in terms of reducing corneal inflammation and progression of herpetic eye disease. These studies will bring much needed benefits to the patients suffering either from the acute infection with high titer of virus favoring the cell-to-cell spread or patient with a chronic immune mediated phase of infection with high infiltrates leading to the scarring of the eye tissues. In addition, multiple clinically relevant viruses potentially use modified versions (2-*O* or 6-*O* or 3-*O*) of sulfated-heparan sulfate (S-HS) during infection (Borst et al., 2013; Kobayashi et al., 2012; Matos et al., 2014), and therefore future testing of SPGG analogs are also vital to investigate the potential for broad-spectrum antiviral activity. Finally, our ability to fine tune the structure of HS-mimetic to generate high-affinity formulations against gD will likely advance the development of a novel drug to maximize the virus inhibition with the better outcomes.

4. Materials and methods

4.1. Chemicals, reagents, and methods

Anhydrous CH_2Cl_2, THF, CH_3OH, CH_3CN, and HPLC grade solvents were purchased from Sigma-Aldrich or Fisher and used as such. All other chemicals were of reaction grade and used as received from Sigma-Aldrich, Fisher, or TCI America. n-Hexylamine for ion-pairing UPLC was from Acros Organics. Analytical TLC was performed using UNIPLATE silica gel GHLF 250 μm precoated plates (ANALTECH).

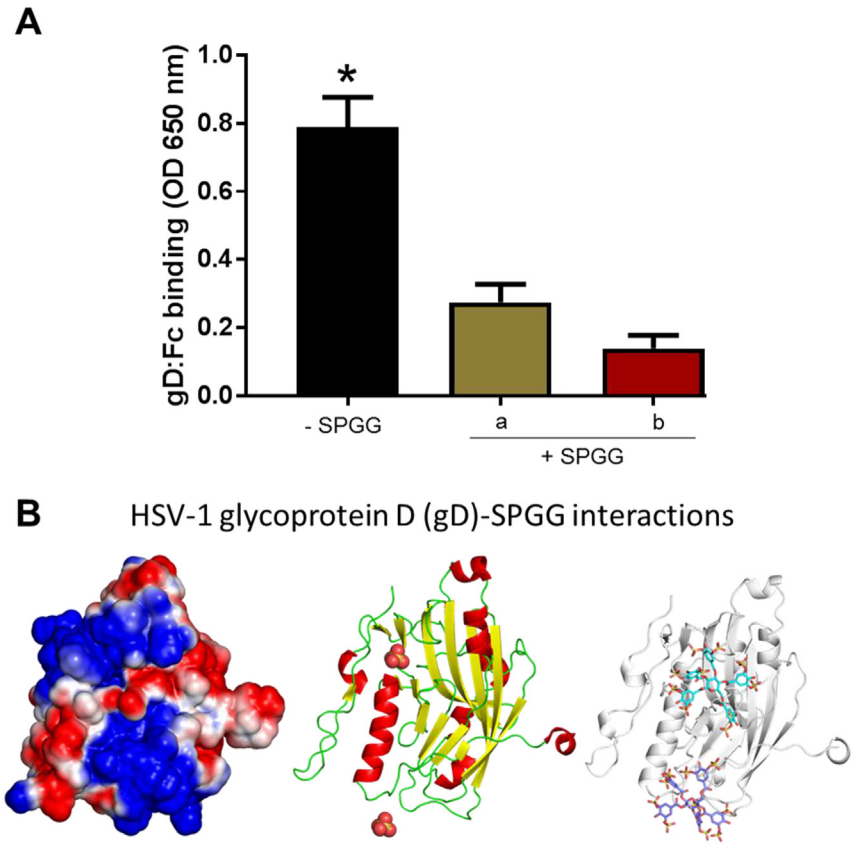

Fig. 7. SPGG impairs HSV-1 gD binding to HIS cells. (A). Cultured HIS were treated with SPGG (10 μM) (bar a) or with PBS buffer for 1 h (positive control). This was followed by incubation with gD-Fc (1 μg/mL) for 1 h and fixation at room temperature with 2% formaldehyde and 0.02% glutaraldehyde for 15 min. In paralle experiment, gD-Fc was pre-incubated with SPGG (bar b) for 1 h followed by fixation (bar b). The cells were washed with PBS containing 3% BSA (Sigma) and then incubated at room temperature sequentially with a biotinylated secondary antibody against rabbit IgG (Sigma) at a 1: 500 dilution in PBS-3% BSA for 45 min and AMDEX streptavidin-conjugated horseradish peroxidase (Amersham) at a 1: 20,000 dilution for 30 min. Following washing in PBS, the cells were incubated with 50 μL 3,3′,5,5′-tetramethylbenzidine (Sigma) in 50 mM phosphate-citrate buffer. Products were quantitated by use of a microplate reader (Thermo Scientific Multiscan FC-96) to measure optical density (OD) at 650 nm. Asterisks indicate significant difference from controls ($P < 0.05$, *t*-test), error bars represent SD from a triplicate experiments. **(B).** Mapping the electrostatic potential surface of gD using APBS tool in PyMol. Blue and red colors represent both electropositive and electronegative surfaces, respectively. The cartoon representation of the structure of gD is shown along with its sulfate groups (present in the crystal structure). The interaction of SPGG with two binding sites on gD is shown as sticks (blue and cyan) respectively.

Column chromatography was performed using silica gel (200–400 mesh, 60 Å) from Sigma-Aldrich. Flash chromatography was performed using Teledyne ISCO, Combiflash RF system and disposable normal silica cartridges of 30–50 μ particle size, 230–400 mesh size, and 60 Å pore size. Sulfated molecules were purified using Sephadex G10 size exclusion chromatography. The quaternary ammonium counterion of sulfate groups present in the molecules was exchanged for sodium ion using SP Sephadex − Na cation exchange chromatography. Each molecule was characterized using ^{1}H and ^{13}C NMR spectroscopy, which was performed on Bruker 400 MHz spectrometer in either $CDCl_3$, CD_3OD, acetone-d_6, or D_2O. ESI MS of unsulfated molecules were recorded using Waters Acquity TQD MS spectrometer in positive ion mode, whereas ESI MS negative mode was used for sulfated compounds.

4.2. Synthesis and characterization of NSGMs

The synthesis and characterization of 3S, SP, SPGG, SG09, SMI, and SCI have been reported earlier (Patel et al., 2014). Briefly, the protected polyphenol precursors of 3S, SPGG, SG09, SMI, and SCI were synthesized by DCC-mediated esterification of glucopyranose scaffold (3S, SPGG, and SG09) or inositol scaffold (SMI and SCI) with tri-benzylated 3,4,5-trihydroxy benzoic acid (SPGG) or di-benzylated 3,5-dihydroxybenzoic acid (3S, SG09, SMI, and SCI). Following esterification, debenzylation-mediated catalytic hydrogenation on Pd-carbon was exploited to give the corresponding polyphenols in quantitative yields. These precursors were then sulfated under microwave conditions using SO_3:$N(CH_3)_3$/Et_3N as the sulfating agent for 6–12 h at 90–100 °C. Each intermediate and final product was characterized using ^{1}H and ^{13}C NMR spectroscopy as well as by UPLC-MS and found to be consistent with the previous reports. Purity of NSGMs was > 95%.

4.3. Cells and viruses

CHO-K1 and CHO Ig8 cells that express β-galactosidase upon viral entry (Montgomery et al., 1996), were grown in Ham's F12 medium (Invitrogen), while HeLa and Vero cells were grown in Dulbecco's modified Eagle medium (DMEM; Invitrogen) supplemented with 10% fetal bovine serum (FBS) and 5% FBS respectively. Cultures of HIS cells derived from the 43 years old female eye donors and obtained from the Illinois Eye Bank, Chicago, IL were used at 7th passage in this study. The procurement of tissues was in accordance with the Declaration of Helsinki. As previously described (Baldwin et al., 2013), HIS cells were grown in l-glutamine-containing DMEM (Invitrogen) supplemented with 15% FBS. Cells were trypsinized and passaged after reaching confluence. Current study used the recombinant β-galactosidase-expressing HSV-1(KOS) gL86 (Shukla et al., 1999), GFP-expressing HSV-1 (K26-GFP) (Desai and Person, 1998), and the wild-type syncytial forming HSV-1 KOS (804) strain (Little and Schaffer, 1981). The viral stocks were propagated at a low multiplicity of infection (MOI) in complementing cell lines, their titers were determined on Vero cells, and they were stored at −80 °C.

4.4. LDH cytotoxicity assay

Primary cultures of HIS cells were plated at optimal cell density (20,000 cells/well) in presence and absence of SPGG at 50 μM. The cell survival was measured by lactate dehydrogenase (LDH) assay, a soluble cytosolic enzyme released from cytoplasm when the membrane becomes leaky after toxic insults. As per manufacture's instruction of the LDH cytotoxicity assay kit (Pierce, Thermo Scientific) 10 × lysis buffer was used for maximum LDH activity controls, while 10 μl sterile water was used a mock treatment for the spontaneous LDH release controls. Following incubation at 24 h, 50 μl supernatant was combined with 50 μl reaction mixture and the plate was incubated at room temperature for 30 min. The LDH activity was determined by measuring the absorbance at 492 nm and 620 nm on Multiskan FC Microplate Photometer and subtracting the 620 nm values from the 492 nm values to remove background. **Viral entry assay.** Viral entry assays were based on

quantification of β-galactosidase expressed from the viral genome in which β-galactosidase expression is inducible by HSV infection (Shukla et al., 1999). Cells were plated at 2×10^4 per well in 96-well plates at least 16 h prior to infection. HSV entry into cells was determined by *o*-nitrophenyl-β-d-galactopyranoside (ONPG) assay and also by 5-bromo-4-chloro-3-indolyl-β-d-galactopyranoside (×-Gal) as previously described (Tiwari et al., 2006). Microscopy was performed with the 20 × objective of an inverted microscope (Axiovert 100 M; Zeiss). All experiments were repeated a minimum of three times unless otherwise noted.

4.5. Counting of viral plaques

Virus replication was examined by counting the plaques in presence of SPGG. A monolayer of cultured HIS (approximately 4×10^6 cells per 25-ml flask) was infected (MOI, 0.01) with HSV-1(KOS) 804 strain or mock infected with PBS alone for 2 h at 37 °C as positive and negative controls, respectively. The HIS cells treated with 10 μM for 1 h before HSV-1 infection. After removal of the inoculum, monolayers were overlaid with DMEM containing 2.5% heat-inactivated calf serum and incubated at 37 °C until the time of harvest (12–48 h). In order to block secondary plaque formation, human immunoglobulin G (IgG; Sigma) was added to the inoculum. The cells were washed with PBS buffer, fixed in alcohol, and stained with Giemsa stain. Infectivity was recorded as the number of plaques formed and imaged in presence and absence of SPGG.

4.6. HSV-1 glycoprotein mediated cell-to-cell fusion assay

In this experiment, the CHO-K1 cells designated effector cells were cotransfected with plasmids expressing four HSV-1(KOS) glycoproteins, pPEP98 (gB), pPEP99 (gD), pPEP100 (gH), and pPEP101 (gL), along with plasmid pT7EMCLuc, which expresses the firefly luciferase gene under the control of the T7 promoter (Tiwari et al., 2004). In parallel wild-type CHO-K1 cells were co-transfected with 3-*O*ST-3 plasmid and T7 RNA Polymerase (Tiwari et al., 2004). A second group cultured HIS cells were also utilized as a target cells were cotransfected with pCAGT7, which expresses T7 RNA polymerase with the chicken actin promoter and the CMV enhancer. Effector cells expressing pT7EMCLuc and pCDNA3 (devoid of any glycoproteins) and target HIS transfected with T7 RNA polymerase alone were used as negative controls. Activation of the reporter luciferase gene, as a measurement of cell fusion in presence and absence of SPGG, was examined by quantitative reporter lysis assay (Promega) and by imaging multinucleated giant cells at 24 h post mixing as previously described (Tiwari et al., 2007).

4.7. Immunofluorescence

SPGG treated or mock treated confluent monolayers of cultured HIS cells (0.5×10^6) on a cover glass (20 by 20 mm; Fisher Scientific, Pittsburgh, PA) were infected with GFP-HSV-1 K26 at 5 MOI at 37 °C. In parallel experiment, HIS cells were pre-incubated with SPGG (50 μM) before HSV-1 infection. After 60 min of infection, cells were washed with phosphate-buffered saline (1 × PBS) and fixed with 4% formalin for 45 min. Fixed cells were then permeabilize with acetone at −20 °C for 5 min followed by staining with tetramethyl rhodamine isocyanate (TRITC)-conjugated phalloidin binding to F-actin as previously described (Tiwari et al., 2008). Finally cells were washed three times with PBS and mounted with Vectashield mounting medium containing DAPI (Vector Laboratories, Inc., Burlingame, CA). Stack microscopy was carried out with Nikon Elements imaging software on a Nikon A1R inverted microscopy system equipped with a 60×, 1.4 numerical aperture oil immersion objective.

4.8. HSV-1 glycoprotein D (gD)-Fc binding assay

Cultured HIS were plated overnight into 96-well dishes (approximately 4×10^4 cells/well). They were treated with SPGG (10 μM) or with PBS buffer as described above for 1 h. In paralle experiment, gD-Fc was pre-incubated with SPGG. This was followed by incubation with gD-Fc (1 μg/mL) for 1 h and fixation at room temperature with 2% formaldehyde and 0.02% glutaraldehyde for 15 min. The cells were washed with PBS containing 3% BSA (Sigma) and then incubated at room temperature sequentially with a biotinylated secondary antibody against rabbit IgG (Sigma) at a 1: 500 dilution in PBS-3% BSA for 45 min and AMDEX streptavidin-conjugated horseradish peroxidase (Amersham) at a 1: 20,000 dilution for 30 min. Following washing in PBS, the cells were incubated with 50 μL 3,3′,5,5′-tetramethylbenzidine (Sigma) in 50 mM phosphate-citrate buffer. Products were quantitated by use of a microplate reader (Thermo Scientific Multiscan FC-96) to measure optical density (OD) at 650 nm.

Acknowledgments

This work was supported by the NIH R01 HL090586 and P01 HL107152 grants to URD and intramural grant support from Midwestern University (MWU) to VT. MWU core-facility for the confocal imaging is kindly acknowledged.

Appendix A. Supplementary data

Supplementary data to this article can be found online at https://doi.org/10.1016/j.antiviral.2018.11.007.

References

Al-Horani, R.A., Desai, U.R., 2014 Jun 12. Designing allosteric inhibitors of factor XIa. Lessons from the interactions of sulfated pentagalloylglucopyranosides. J. Med. Chem. 57 (11), 4805–4818. https://doi.org/10.1021/jm500311e. Epub 2014 May 29.

Al-Horani, R.A., Ponnusamy, P., Mehta, A.Y., Gailani, D., Desai, U.R., 2013 Feb 14. Sulfated pentagalloylglucoside is a potent, allosteric, and selective inhibitor of factor XIa. J. Med. Chem. 56 (3), 867–878. https://doi.org/10.1021/jm301338q. Epub 2013 Jan 28.

Al-Horani, R.A., Gailani, D., Desai, U.R., 2015 Aug. Allosteric inhibition of factor XIa. Sulfated non-saccharide glycosaminoglycan mimetics as promising anticoagulants. Thromb. Res. 136 (2), 379–387. https://doi.org/10.1016/j.thromres.2015.04.017. Epub 2015 Apr 22.

Atanasiu, D., Saw, W.T., Cohen, G.H., Eisenberg, R.J., 2010 Dec. Cascade of events governing cell-cell fusion induced by herpes simplex virus glycoproteins gD, gH/gL, and gB. J. Virol. 84 (23), 12292–12299.

Baldwin, J., Park, P.J., Zanotti, B., Maus, E., Volin, M.V., Shukla, D., Tiwari, V., 2013 Apr. Susceptibility of human iris stromal cells to herpes simplex virus 1 entry. J. Virol. 87 (7), 4091–4096. https://doi.org/10.1128/JVI.03235-12. Epub 2013 Jan 23.

Borst, E.M., Ständker, L., Wagner, K., Schulz, T.F., Forssmann, W.G., Messerle, M., 2013 Oct. A peptide inhibitor of cytomegalovirus infection from human hemofiltrate. Antimicrob. Agents Chemother. 57 (10), 4751–4760 PMID: 23856778.

Dawson, C.R., Togni, B., 1976. Herpes simplex eye infections: clinical manifestations, pathogenesis and management. Surv. Ophthalmol. 21, 121–135.

Desai, U.R., 2013 Aug. The promise of sulfated synthetic small molecules as modulators of glycosaminoglycan function. Future Med. Chem. 5 (12), 1363–1366. https://doi.org/10.4155/fmc.13.117.

Desai, P., Person, S., 1998 Sep. Incorporation of the green fluorescent protein into the herpes simplex virus type 1 capsid. J. Virol. 72 (9), 7563–7568 PMID: 9696854.

Dredge, K., Hammond, E., Davis, K., Li, C.P., Liu, L., Johnstone, K., Handley, P., Wimmer, N., Gonda, T.J., Gautam, A., Ferro, V., Bytheway, I., 2010 Jun. The PG500 series: novel heparan sulfate mimetics as potent angiogenesis and heparanase inhibitors for cancer therapy. Invest. N. Drugs 28 (3), 276–283.

Eisenberg, R.J., Atanasiu, D., Cairns, T.M., Gallagher, J.R., Krummenacher, C., Cohen, G.H., 2012. Herpes virus fusion and entry: a story with many characters. Viruses 4, 800–832.

Ferro, V., Dredge, K., Liu, L., Hammond, E., Bytheway, I., Li, C., Johnstone, K., Karoli, T., Davis, K., Copeman, E., Gautam, A., 2007 Jul. PI-88 and novel heparan sulfate mimetics inhibit angiogenesis. Semin. Thromb. Hemost. 33 (5), 557–568.

Fischer, N.O., Mbuy, G.N., Woodruff, R.I., 2001. HSV-2 disrupts gap junctional intercellular communication between mammalian cells in vitro. J. Virol Methods 91, 157–166.

Gangji, R.N., Sankaranarayanan, N.V., Elste, J., Al-Horani, R.A., Afosah, D.K., Joshi, R., Tiwari, V., Desai, U.R., 2018 Jul 16. Inhibition of herpes simplex virus-1 entry into human cells by nonsaccharide glycosaminoglycan mimetics. ACS Med. Chem. Lett. 9

(8), 797–802.
Herold, B.C., WuDunn, D., Soltys, N., Spear, P.G., 1991. Glycoprotein C of herpes simplex virus type 1 plays a principal role in the adsorption of virus to cells and in infectivity. J. Virol. 65, 1090–1098.
Jayson, G.C., Miller, G.J., Hansen, S.U., Barath, M., Gardiner, J.M., Avizienyte, E., 2014 Dec. The development of anti-angiogenic heparan sulfate oligosaccharides. Biochem. Soc. Trans. 42 (6), 1596–1600. https://doi.org/10.1042/BST20140229.
Kobayashi, F., Yamada, S., Taguwa, S., Kataoka, C., Naito, S., Hama, Y., Tani, H., Matsuura, Y., Sugahara, K., 2012. Specific interaction of the envelope glycoproteins E1 and E2 with liver heparan sulfate involved in the tissue tropismatic infection by hepatitis C virus. Glycoconj. J. 29 (4), 211–220 PMID: 22660965.
Krummenacher, C., Carfí, A., Eisenberg, R.J., Cohen, G.H., 2013. Entry of herpesviruses into cells: the enigma variations. Adv. Exp. Med. Biol. 790, 178–195.
Little, S.P., Schaffer, P.A.A., 1981. Expression of the syncytial (syn) phenotype in HSV-1, strain KOS: genetic and phenotypic studies of mutants in two syn loci. Virology 112, 686–702.
Matos, P.M., Andreu, D., Santos, N.C., Gutiérrez-Gallego, R., 2014. Structural requirements of glycosaminoglycans for their interaction with HIV-1 envelope glycoprotein gp120. Arch. Virol. 159 (3), 555–560 PMID: 24046088.
Montgomery, R.I., Warner, M.S., Lum, B.J., Spear, P.G., 1996. Herpes simplex virus-1 entry into cells mediated by a novel member of the TNF/NGF receptor family. Cell 87, 427–436.
Oh, M.J., Akhtar, J., Desai, P., Shukla, D., 2010 Jan 1. A role for heparan sulfate in viral surfing. Biochem. Biophys. Res. Commun. 391 (1), 176–181.
Patel, N.J., Karuturi, R., Al-Horani, R.A., Baranwal, S., Patel, J., Desai, U.R., Patel, B.B., 2014 Aug 15. Synthetic, non-saccharide, glycosaminoglycan mimetics selectively target colon cancer stem cells. ACS Chem. Biol. 9 (8), 1826–1833. https://doi.org/10.1021/cb500402f. Epub 2014 Jun 26.
Raman, K., Karuturi, R., Swarup, V.P., Desai, U.R., Kuberan, B., 2012 Jul 1. Discovery of novel sulfonated small molecules that inhibit vascular tube formation. Bioorg. Med. Chem. Lett 22 (13), 4467–4470. https://doi.org/10.1016/j.bmcl.2012.04.014. Epub 2012 Apr 16.
Rathinam, S.R., Namperumalsamy, P., 2007. Global variation and pattern changes in epidemiology of uveitis. Indian J. Ophthalmol. 55, 173–183.
Sattentau, Q., 2008. Avoiding the void: cell-to-cell spread of human viruses. Nat. Rev. Microbiol. 6, 815–826.
Sheng, G.J., Oh, Y.I., Chang, S.K., Hsieh-Wilson, L.C., 2013 Jul 31. Tunable heparan sulfate mimetics for modulating chemokine activity. J. Am. Chem. Soc. 135 (30), 10898–10901. https://doi.org/10.1021/ja4027727. Epub 2013 Jul 23.
Shieh, M.T., WuDunn, D., Montgomery, R.I., Esko, J.D., Spear, P.G., 1992 Mar. Cell surface receptors for herpes simplex virus are heparan sulfate proteoglycans. J. Cell Biol. 116 (5), 1273–1281.
Shukla, D., Spear, P.G., 2001 Aug. Herpesviruses and heparan sulfate: an intimate relationship in aid of viral entry. J. Clin. Invest. 108 (4), 503–510.
Shukla, D., Liu, J., Blaiklock, P., Shworak, N.W., Bai, X., Esko, J.D., Cohen, G.H., Eisenberg, R.J., Rosenberg, R.D., Spear, P.G., 1999. A novel role for 3-O-sulfated heparan sulfate in herpes simplex virus 1 entry. Cell 99, 13–22.
Spear, P.G., Longnecker, R., 2003. Herpesvirus entry: an update. J. Virol. 77, 10179–10185.
Sungur, G.K., Hazirolan, D., Yalvac, I.S., Ozer, P.A., Aslan, B.S., Duman, S., 2010. Incidence and prognosis of ocular hypertension secondary to viral uveitis. Int. Ophthalmol. 30, 191–194.
Teitelbaum, C.S., Streeten, B.W., Dawson, C.R., 1987. Histopathology of herpes simplex virus keratouveitis. Curr. Eye Res. 6, 189–194.
Tiwari, V., Clement, C., Duncan, M.B., Chen, J., Liu, J., Shukla, D., 2004 Apr. A role for 3-O-sulfated heparan sulfate in cell fusion induced by herpes simplex virus type 1. J. Gen. Virol. 85 (Pt 4), 805–809.
Tiwari, V., Clement, C., Xu, D., Valyi-Nagy, T., Yue, B.Y., Liu, J., Shukla, D., 2006 Sep. Role for 3-*O*-sulfated heparan sulfate as the receptor for herpes simplex virus type 1 entry into primary human corneal fibroblasts. J. Virol. 80 (18), 8970–8980.
Tiwari, V., ten Dam, G.B., Yue, B.Y., van Kuppevelt, T.H., Shukla, D., 2007 Sep 18. Role of 3-O-sulfated heparan sulfate in virus-induced polykaryocyte formation. FEBS Lett. 581 (23), 4468–4472 Epub 2007 Aug 24.
Tiwari, V., Oh, M.J., Kovacs, M., Shukla, S.Y., Valyi-Nagy, T., Shukla, D., 2008 Nov. Role for nectin-1 in herpes simplex virus 1 entry and spread in human retinal pigment epithelial cells. FEBS J. 275 (21), 5272–5285 PMID: 18803666.
Tiwari, V., Liu, J., Valyi-Nagy, T., Shukla, D., 2011 Jul 15. Anti-heparan sulfate peptides that block herpes simplex virus infection in vivo. J. Biol. Chem. 286 (28), 25406–25415. https://doi.org/10.1074/jbc.M110.201103. Epub 2011 May 19.
Todd, Wuest, Zheng, Min, Efstathiou, Stacey, Halford, William P., Daniel, J., Carr, J., 2011 October. The Herpes Simplex Virus-1 Transactivator Infected Cell Protein-4 Drives VEGF-A Dependent Neovascularization. PLoS Pathog. 7 (10), e1002278.
Tugal-Tutkun, I., Ötük-Yasar, B., Altinkurt, E., 2010. Clinical features and prognosis of herpetic anterior uveitis: a retrospective study of 111 cases. Int. Ophthalmol. 30, 559–565.
Van der Lelij, A., Ooijman, F.M., Kijlstra, A., Rothova, A., 2000. Anterior uveitis with sectoral iris atrophy in the absence of keratitis: a distinct clinical entity among herpetic eye diseases. Ophthalmology 107, 1164–1170.
West, Devin M., Del Rosso, Chelsea R., Yin, Xiao-Tang, Patrick, M., Stuart, 2014 February 15. CXCL1, but not IL-6 is required for recurrent herpetic stromal keratitis. J. Immunol. 192 (4), 1762–1767.
Wilson, Sarah S., Fakioglu, Esra, Herold, Betsy C., 2009 June. Novel approaches in fighting herpes simplex virus infections Expert Rev Anti Infect Ther. Author manuscript; available in PMC 2010 April 1. Published in final edited form as. Expert Rev. Anti Infect. Ther. 7 (5), 559–568.
WuDunn, D., Spear, P.G., 1989 Jan. Initial interaction of herpes simplex virus with cells is binding to heparan sulfate. J. Virol. 63 (1), 52–58.
Zhu, L., Zhu, H., 2014 Dec. Ocular herpes: the pathophysiology, management and treatment of herpetic eye diseases. Virol. Sin. 29 (6), 327–342.